Energy Conversion and Management 351 (2026) 121003

Contents lists available at ScienceDirect

Energy Conversion and Management

journal homepage: www.elsevier.com/locate/enconman

Research Paper

Weather-dependent direct air capture process modeling for techno-economic assessments

Aaron S. Jajjawi [a,b,*], Henrik Wenzel [c,d], Freia Harzendorf [c], Jann M. Weinand [c], Detlef Stolten [d], Ralf Peters [a,b]

[a] Forschungszentrum Jülich GmbH, Institute of Energy Technologies – Electrochemical Process Engineering (IET-4), 52425 Jülich, Germany
[b] Ruhr-University Bochum, Synthetic Fuels, Faculty of Mechanical Engineering, 44780 Bochum, Germany
[c] Forschungszentrum Jülich GmbH, Institute of Climate and Energy Systems – Jülich Systems Analysis (ICE-2), 52425 Jülich, Germany
[d] RWTH Aachen University, Chair for Fuel Cells, Faculty of Mechanical Engineering, 52062 Aachen, Germany

ARTICLE INFO

Keywords:
Co-adsorption
Temperature-vacuum-swing-adsorption
Process optimization
Coupled process-cost evaluation

ABSTRACT

Adsorption-based Direct Air Capture (DAC) is crucial for achieving negative emissions but faces significant challenges due to high energy demand and operational costs. While recent research has highlighted that weather conditions significantly affect DAC energy demand and cost, current DAC systems are typically optimized under steady-state conditions, overlooking the impact of ambient weather variability on the optimal operating point. This study addresses that gap by investigating whether dynamically adjusted adsorption and desorption durations based on hourly weather conditions can improve energy efficiency compared to static operation. Therefore, a process model incorporating co-adsorption effects was optimized for real-world weather conditions and the results are utilized as an input for a techno-economic assessment. Dynamic operation of the optimized process model was evaluated using hourly weather data from four possible DAC locations, revealing potential reductions in electrical and thermal energy demands of up to 8.8 % and 0.9 %, respectively. Additional analyses show that simplified day–night and seasonal operating strategies achieve nearly the same energy savings as hourly adaptation, substantially reducing control complexity. Integration of the optimized process model into a techno-economic assessment reveals weather-driven cost variations of up to 72 €/t_{CO2} and demonstrates strong sensitivity of DAC costs to renewable energy intermittency. By providing detailed data on the optimized process model, including energy consumption and productivity across diverse climatic conditions, the study supports more refined and location-specific future assessments.

1. Introduction

1.1. Background and context

According to the Intergovernmental Panel on Climate Change, the deployment of Negative Emission Technologies (NETs) will be necessary to limit the global mean temperature rise to 2 °C or below [1]. Even under ambitious mitigation pathways, fully eliminating emissions across globally interconnected supply chains remains challenging. Factors such as CO_2 pricing, energy availability, and operational uncertainties continue to restrict decarbonization efforts and limit the feasibility of complete emission abatement [2–5]. Consequently, residual emissions will persist, particularly in sectors with limited abatement options. Among the available NETs, Direct Air Capture (DAC) offers verifiable and location-independent removal of atmospheric CO_2, positioning it as an important complement to conventional mitigation strategies [6].

First commercial DAC plants are already in operation, demonstrating the technical feasibility of the employed adsorption technology [7]. However, the high energy demand and associated costs continue to limit large-scale deployment. Research on DAC spans multiple disciplines, such as sorbent material development, regional deployment strategies, regulatory frameworks, and life-cycle assessments, as recently shown by Harzendorf et al. and van der Spek et al. [8,9]. Within this broader context, improving the efficiency and economic performance of adsorption-based DAC remains a key challenge.

Currently, the only commercially available adsorbent specifically

* Corresponding author at: Forschungszentrum Jülich GmbH, Institute of Energy Technologies – Electrochemical Process Engineering (IET-4), 52425 Jülich, Germany.
E-mail address: a.jajjawi@fz-juelich.de (A.S. Jajjawi).

https://doi.org/10.1016/j.enconman.2025.121003
Received 9 July 2025; Received in revised form 15 December 2025; Accepted 25 December 2025
Available online 7 January 2026

developed for DAC applications is Lewatit® VP OC 1065, an amine-functionalized polymer resin. A key characteristic of such materials is their strong interaction with water vapor, which significantly affects CO_2 capture performance. Although a multi-component adsorption is inherently competitive, many studies report the enhancing effect of co-adsorbed water on the CO_2 capacity of the adsorbent [10–12]. Recent work suggests that this enhancement arises primarily from physical effects, such as polymer swelling, which facilitates CO_2 transport within the adsorbent [13]. The magnitude of this effect depends on humidity and the competitive nature of multicomponent adsorption [10,14–16]. Because of these complex interactions, the net capacity increase is expected to vary significantly with ambient humidity, which makes it an important consideration for DAC systems operating under atmospheric conditions. To this end, only a limited number of studies have developed and integrated co-adsorption models into process models [17–23].

Low-temperature DAC processes require a combination of heat input and pressure reduction to achieve meaningful CO_2 working capacities [10,24–26]. With adsorption performed near ambient conditions, vacuum levels are needed to enable efficient desorption [27]. Hence, adsorption-based DAC systems typically operate cyclically in a temperature–vacuum swing adsorption (TVSA) process [24,28]. The process is referred to as steam-assisted temperature-vacuum swing adsorption (S-TVSA), if the required heat is supplied via direct steam injection into the adsorption column [28]. The choice of desorption temperature in low-temperature DAC processes, which generally lies between 80 °C and 130 °C [9], is influenced by both the available thermal energy source and the temperature stability of the sorbent material [29]. In the case of Lewatit® VP OC 1065, the manufacturer specifies a maximum operating temperature of 100 °C [30], making it particularly well-suited for heat pump integration [31,32]. This compatibility with low-temperature heat is a notable advantage for energy supply concepts, especially in the context of renewable integration.

In addition to sorbent properties and heat-supply strategy, the cycle configuration is a critical lever for performance optimization. The optimal operating point of the process shifts over time, given that ambient temperature and humidity strongly influence CO_2 capture efficiency and vary over time [12,17,18]. Weather-adaptive cycle control could therefore improve efficiency compared to static operation with fixed cycle settings, potentially reducing both energy demand and costs.

2. Research gap and significance

While most DAC optimization studies assume steady-state or fixed ambient conditions, a limited number of contributions have begun exploring process performance under varying climatic conditions. Sendi et al. [17] incorporated weather-resolved data into an S-TVSA system and demonstrated notable differences in energy requirements and costs. However, the study assumed static operation and did not investigate dynamic control strategies or their impact on process and economic performance. Wiegner et al. [18] optimized an adsorption-based DAC system for productivity across different climate zones but did not incorporate a co-adsorption model or weather variability on sub-daily timescales. Additionally, the examined temperature range was limited to 5–40 °C. Postweiler et al. [21] evaluated DAC operation with a focus on carbon removal efficiency, but used a non-commercial adsorbent, which hinders comparability and experimental validation. Rezo et al. [22] applied the adsorbent model introduced by Postweiler et al. [21] and coupled a dynamic process model with weather data, focusing on siting strategies in Europe. Their work addressed seasonal energy balancing and did not explore short-term operational flexibility. In parallel, several techno-economic assessments have analyzed global DAC siting or future energy supply scenarios [33–35]. However, techno-economic assessments without an adequately detailed process model introduce uncertainty since the model output is not fully tailored to economic evaluation. An overview of the relevant studies is provided in Table 1.

It becomes clear that much of the existing DAC literature either employs adsorbent models without experimentally validated co-adsorption behavior or relies on non-commercial materials. Both factors limit reproducibility and hinder meaningful experimental benchmarking. Furthermore, the incorporation of weather variability into DAC process models is either neglected or restricted to coarse temporal resolution, despite the strong impact of ambient temperature and humidity on adsorption performance. In addition, most studies assume static operation, overlooking the potential of dynamically adjusting cycle parameters in response to environmental fluctuations. Finally, the data generated by process models is commonly not tailored toward techno-economic assessment, resulting in inconsistencies and uncertainties when performance metrics are transferred into a system-level evaluation.

To address these research gaps, this work develops a detailed one-dimensional TVSA process model incorporating a validated co-adsorption model for a commercially available sorbent. The model is used to simulate DAC operation under hourly-resolved climate conditions and to identify weather-adapted, dynamic operating strategies that enhance process efficiency. The resulting performance indicators, including specific energy demand, productivity, and water co-adsorption, are directly formulated to ensure seamless integration into a robust techno-economic assessment. Using this unified modeling framework, the influence of weather variability and operational flexibility on DAC performance is quantified across multiple global locations and translated into corresponding CO_2 removal costs.

Table 1
Comprehensive overview of recent literature involving DAC process modelling.

Study	Co-adsorption modeling	Weather data input	Dynamic DAC operation	Economic evaluation	Main limitations
Sendi et al., [17]	Yes	Yes	No, static operation	Yes	No dynamic weather response
Wiegner et al., [18]	No	Yes, no hourly resolution	Yes, different operation strategies	Yes	No co-adsorption, no dynamic weather response
Postweiler et al., [21]	Yes, proprietary adsorbent	No	No, static operation	No	No benchmark adsorbent, no dynamic DAC, no TEA
Rezo et al., [22]	Yes, proprietary adsorbent	Yes	No, static operation	No	Lacks short-term flexibility, no TEA
Zhang et al., [23]	Yes	No	No, static operation	No	No weather data integration or TEA
Terlouw et al., [33]	No (Wiegner model)	Yes	No	Yes	No co-adsorption, no dynamic weather response
Sendi et al., [34]	Not disclosed	Yes	No	Yes	No dynamic weather response
Wenzel et al., [35]	Yes	Yes	No	Yes	No dynamic weather response

2.1. Objective and scope

The objective of this study is to evaluate the performance and economic implications of weather-dependent operation of a low-temperature TVSA DAC process using a commercially available amine-functionalized sorbent. To achieve this objective, the study:

- develops a detailed TVSA process model in Aspen Adsorption incorporating a validated co-adsorption model for Lewatit® VP OC 1065,
- simulates DAC operation under hourly-resolved temperature and humidity conditions at multiple global locations,
- identifies dynamic operating strategies (fully dynamic, seasonal cycles, day-night cycles) that adapt cycle parameters to changing weather conditions, and
- provides techno-economic performance metrics, directly derived from the process model, to quantify the influence of weather variability on CO_2 removal costs.

The scope of the study is limited to stand-alone adsorption-based DAC operation using low-temperature heat. Broader system-level integration aspects such as supply chain logistics, energy infrastructure constraints, and environmental impact assessments are outside the scope of this work.

2.2. Structure of the paper

The remainder of this paper is organized as follows. Section 2 describes the methodology, including the development of the TVSA process model, the implementation of the co-adsorption formulation, the use of hourly weather data, and the techno-economic evaluation framework. Section 3 presents the results of the weather-resolved process simulations and the dynamic operation strategies, as well as their impact on CO_2 removal costs at different locations. Section 4 discusses these findings in the context of DAC deployment, highlights limitations, and provides conclusions and recommendations for future work.

3. Methodology

This section begins by providing a detailed description of the developed process model, followed by the definition of KPIs relevant to DAC system evaluation. The subsequent part outlines the optimization approach used to derive weather-dependent operating parameters. Finally, the methodology and underlying assumptions employed in the techno-economic assessment are presented.

3.1. Thermodynamic modeling

Aspen Adsorption has been used in only a limited number of DAC-related modeling studies [23,36], but its structured simulation environment offers several advantages that motivated its use in this study. The software enables dynamic modeling of cyclic adsorption processes and supports the convergence to cyclic steady state under varying boundary conditions. It provides access to validated heat- and mass-transfer correlations and pressure-drop models that can be adapted for DAC operating regimes. The integrated Aspen Properties Database ensures consistency in thermophysical data, while the time-resolved solution allows detailed evaluation of transient behavior during individual cycle steps. Furthermore, the model structure and parameter definitions are fully transparent and reproducible, supporting rigorous scientific assessment and comparison with future studies [37].

3.2. Material properties, adsorption models, and kinetic expression

Lewatit® VP OC 1065 is used as the adsorbent in this study. It is a primary-amine functionalized polymer resin supplied as spherical beads [30,38]. and widely established as a benchmark material for adsorption-based DAC systems. Its thermophysical properties and adsorption behavior under ambient DAC conditions have been extensively characterized in literature, providing a reliable foundation for process modeling [12,15,36,38,39]. The material properties used in this work are summarized in Table 4 in the Supplementary Information (SI).

In addition to CO_2 uptake, water co-adsorption plays a significant role in DAC operation. The amount of adsorbed water depends strongly on ambient temperature and relative humidity and has been shown to enhance CO_2 adsorption. Recent findings indicate that this enhancement primarily arises from physical effects such as polymer swelling, which improves intra-particle CO_2 transport, rather than changes in amine chemistry [13]. To accurately capture this behavior, the weighted-average dual-site Toth (WADST) co-adsorption model developed by Young et al. [12] is implemented in Aspen Adsorption. All employed parameters are presented in Table 1 of the SI.

A number of studies underline the importance of including isotherms for nitrogen (N_2) and oxygen (O_2) adsorption in thermodynamic models, however, applicable and cohesive adsorption models are not available literature [28]. For this reason, N_2 and O_2 adsorption is not included in the thermodynamic model and, therefore, remain as inert species in the gas phase.

The expression of the employed co-adsorption model of CO_2 is based on the Toth isotherm and is expressed as shown in equation (1).

$$q_{CO_2} = \left(1 - exp\left(-\frac{A}{q_{H_2O}}\right)\right) \bullet \frac{q_{CO_2max} \bullet K(T) \bullet p_{CO_2}}{\left(1 + \left(K(T) \bullet p_{CO_2}\right)^{b(T)}\right)^{1/b(T)}} + \left(exp\left(-\frac{A}{q_{H_2O}}\right)\right) \bullet \frac{q_{CO_2max,wet} \bullet K_{wet}(T) \bullet p_{CO_2}}{\left(1 + \left(K_{wet}(T) \bullet p_{CO_2}\right)^{b_{wet}(T)}\right)^{1/b_{wet}(T)}} \quad (1)$$

where q_{CO_2} is the loading of CO_2, A is a factor for the Arrhenius expression, q_{H_2O} is the loading of water, and q_{CO_2max} is the maximum CO_2 loading at dry and wet conditions, respectively. Furthermore, the affinity parameter K at dry and wet conditions, the CO_2 partial pressure p_{CO_2} and the surface heterogeneous factor under dry and wet conditions b are needed. The values of all parameters are stated in Table 1 in the SI. The water isotherm is taken from the study of Young et al. [12] and expressed by a temperature-dependent Guggenheim-Anderson-de Boer (GAB) model (see Table 2 in the SI).

The kinetic model consists of a lumped resistance on the solid surface in the form of a linear driving force (LDF) model. It is expressed as a function of the equilibrium loading, calculated by Aspen Adsorption and the actual loading of a species at a given timestep (see equation (2)). The mass transfer coefficients are also adopted from the study of Young et al. [12] to obtain a cohesive thermodynamic model.

Table 2
Description and units of variables used in the KPI calculations.

Symbol	Description	Unit
$\dot{V}_{Air}$	Air volumetric flowrate at inlet	m^3/s
Δp	Pressure drop across adsorption bed	Pa
η_{fan}	Fan efficiency	–
$\dot{n}$	Molar flowrate of desorbate	mol/s
R	Gas constant	J/mol/K
T	Temperature at desorption outlet	K
η_{VP}	Vacuum pump efficiency	–
p_H	High pressure during desorption	Pa
p_L	Low (vacuum) pressure during desorption	Pa
$m_{CO_2,produced}$	CO_2 mass collected per cycle	kg or t_{CO2}
$\dot{m}_{Flow}$	Heating fluid mass flowrate	kg/s
c_p	Gas heat capacity	J/kg/K
dT_{HEx}	Heat exchanger temperature	K
z	Column length	m
t_{Cycle}	Duration of full cycle	s

$$\frac{\partial q_k}{\partial t} = MTC_k\left(q_k^* - q_k\right), k = CO_2, H_2O \quad (2)$$

Where q_k is the loading of a component, MTC_k is the mass transfer coefficient of a component, and q_k^* is the equilibrium loading of a component for a given adsorption condition. All parameters are specified in the SI (see Table 3 in the SI). The fundamental process equations used in this study are based on the built-in models and correlations provided by Aspen Adsorption [40].

3.3. Mass, energy, and momentum balances

The mass balance includes convection, axial dispersion and mass transfer between gas and solid phase. For the gas phase, the mass balance is defined for each substance k as shown in equation (3):

$$-\varepsilon_i E_{z,k}\frac{\partial^2 c_k}{\partial z^2} + \frac{\partial\left(v_g c_k\right)}{\partial z} + \varepsilon_B\frac{\partial c_k}{\partial t} + J_k = 0 \quad (3)$$

The first term describes axial dispersion including the second derivative of the concentration with respect to the axial position, for which the dispersion coefficient for a component is determined by Aspen Adsorption (see SI). The second term describes convection including the derivate of the product of gas velocity and concentration with respect to the axial position. The third term describes the accumulation of species in the gas phase including the time derivate of the concentration. The fourth term describes the rate of mass transfer of component k from the gas phase to the solid surface per unit volume of the bed. It expresses the adsorption and desorption dynamics. The molecular diffusivities required to determine the dispersion coefficients are assumed to be constant. The ideal gas law is applied to the system. More information on the mass balance is provided in section 1.5 in the SI Table 4.

The energy balance is modeled for a non-isothermal adsorption column with gas and solid conduction. Therefore, the complete energy balance consists of expressions for the energy balances of the gas and solid phase. The adsorbed phase heat capacities, the heats of adsorption, the heat transfer coefficient between gas and solid phase, gas thermal conductivity and the solid phase heat capacity are assumed to be constant. The column is modelled adiabatically. The energy balance for the gas phase is expressed in eq. (4).

$$-\varepsilon_i k_g\frac{\partial^2 T_g}{\partial z^2} + C_{vg}v_g\rho_g\frac{\partial T_g}{\partial z} + \varepsilon_B C_{vg}\rho_g\frac{\partial T_g}{\partial z} + HTC \bullet a_p\left(T_g - T_s\right) + a_{Hx}Q_{Hx} = 0 \quad (4)$$

The first term represents axial thermal conduction (axial thermal dispersion) in the gas phase, followed by the convective heat transport term. The third term accounts for enthalpy accumulation in the gas phase, while the fourth term expresses heat transfer. The fifth term describes heat exchange between the gas phase and an external heat exchanger (jacket). More information on the corresponding energy balance for the solid phase, as well as a thorough explanation of the terms and parameters is provided in section 1.6 and Table 5 in the SI.

The momentum balance is modeled considering the Ergun equation (see section 1.7 in the SI).

Table 3
Overview of variables excluded from the optimization routine.

Variable	Value	Comment
Air flow rate $\dot{V}_{air}$	6.2 $\frac{L}{s}$	This air flow rate results in a pressure loss of 200 Pa in the adsorption bed during adsorption, which aligns with design recommendations given by Wu et al. [44].
Desorption temperature T_{des}	90 °C	At this temperature, the adsorption column can be heated using hot water and the adsorbent is stable.
Desorption pressure p_{des}	0.1 bar	Most DAC applications and models employ a coarse vacuum pressure during desorption, as it offers a technically straightforward implementation.
Evacuation time t_{eva}	60 s	Model assumption
Cooling time t_{cool}	600 s	Model calculation considering a cooling water temperature of 10 °C

Table 4
Utilized techno-economic parameters for the energy system in the PV supply scenario.

	CAPEX	OPEX	Further aspects	Based on
		%$_{CAPEX}$/a		
OFPV	1276 €/kW	1.6		[53]
Battery	405 €/kWh	2.5	4-hour battery with round-trip efficiency of 85 %	[53]
Heat pump	832 €/kW$_{th}$	0.5	Coefficient of performance = 2	[31]
Electric Heater	151 €/kW$_{th}$	0.4		[54]

3.4. Process description

The single adsorption bed is a flat packed bed containing the employed adsorbent. For this study, a small- scale DAC test plant is simulated. It has a diameter of 10 cm and a bed height of 2 cm. A flat design for the adsorption bed is used by most researchers and pilot plants which employ a bead-shaped adsorbent like Lewatit® VP OC 1065 to avoid high pressure drops [11,41]. Heat is supplied by a heating jacket installed around the adsorption chamber (see Fig. 1).

The adsorption chamber is equipped with multiple inlet and outlet valves that control the gas flow and pressure. During adsorption, ambient air enters at the bottom of the column, passes through the packed bed, and CO_2-depleted air exits at the top. During desorption, these ports are closed, and a dedicated valve at the column top is opened to first evacuate the residual air and later withdraw the product gas.

The operating cycle consists of four steps:

(1) **Adsorption**: Air containing 400 ppm CO_2 flows through the column, and CO_2 and water vapor are selectively adsorbed. When the target CO_2 loading is reached, the airflow is stopped.
(2) **Evacuation**: The column is depressurized to 0.1 bar to remove residual gas from the void space. This prevents oxidative degradation of the sorbent and enables production of a purer desorption stream.
(3) **Desorption**: Once the target vacuum level is established, the heating jacket is activated. The bed temperature rises toward the desorption setpoint, and CO_2 and water desorb from the sorbent. Desorption ends when the residual loading reaches the defined cut-off value.
(4) **Cooling**: The column is isolated and cooled via the heating jacket operating in cooling mode. The bed temperature must fall below 75 °C before repressurization to avoid oxidative degradation of the amine functionalities during the subsequent adsorption step [42].

3.5. Process model assumptions

The assumption of adiabatic operation with constant effective thermal properties idealizes heat transfer within the adsorption column. In practical systems, heat losses and non-uniform heat transfer may increase the absolute thermal energy demand; however, the relative difference between static and dynamic operation is expected to remain similar, since both strategies are affected to a comparable extent. Furthermore, existing patented adsorption chamber designs typically

Table 5
Optimal adsorption and desorption duration of all climate cluster points.

Cluster	Temperature	Relative humidity	Adsorption duration	Desorption duration	Specific total energy demand
	°C	%	min	min	MWh/t_{CO2}
1	16	44	38	70.5	2.80
2	9	83	28	82	3.95
3	22	17	36	63	2.83
4	13	71	33	79.5	3.51
5	26	69	36	77.5	3.71
6	−4	87	26	79	3.82
7	29	40	41	70.5	2.95
8	12	93	24	83	4.42
9	5	27	38	69	2.54
10	23	94	25	83.5	4.85
11	1	94	24	83	4.26
12	−2	75	29	79.5	3.54
13	14	58	36	76	3.13
14	27	55	42	75	3.26
15	19	31	39	68.5	2.64
16	31	26	38	66	2.97
17	24	82	31	81.5	4.28
18	35	13	31	58	4.24
19	0	62	32	77	3.19
20	1	46	37	74	2.81
21	−10	5	30	57.5	4.17
22	50	100	24	82.5	6.97

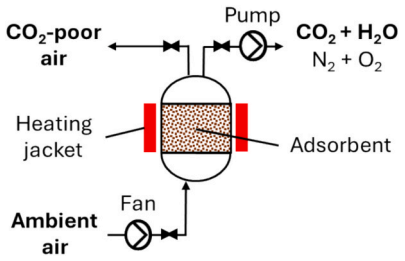

Fig. 1. Schematic diagram of the DAC process modeled in this study. Adsorption takes place inside the adsorption chamber, which contains a cylindrical packed bed filled with the adsorbent Lewatit® VP OC 1065.

include insulation to minimize heat losses, supporting the applicability of the adiabatic assumption [43].

The LDF model used for intraparticle mass transfer represents a lumped approximation that does not resolve internal pore diffusion gradients explicitly. This simplification may lead to deviations in transient uptake behavior, particularly since water and CO_2 exhibit different diffusivities within amine-functionalized adsorbents. However, co-adsorption behavior in this system is largely determined by thermodynamic competition rather than rate limitations, suggesting that the relative impact of humidity on working capacity trends is captured reliably. More detailed pore-scale diffusion formulations could be incorporated in future work to further quantify transport–reaction interactions under dynamic operating conditions.

The reactor geometry used in this study represents a laboratory-scale fixed-bed configuration. At pilot or commercial scale, larger characteristic dimensions may introduce additional transport effects, including radial thermal gradients, non-uniform humidity profiles, and increased pressure drop. These scale-dependent behaviors can be interpreted through standard dimensionless numbers. Although a dimensionless similarity analysis is beyond the scope of this study. The operating conditions modeled here lie in the same general transport regime expected for industrial DAC beds, where external film resistances remain small compared to intraparticle limitations. Industrial TVSA DAC modules are also expected to employ internal heat exchangers rather than external wall heating. Provided that the heat-exchange surface area per unit bed volume is preserved, the overall thermal regeneration efficiency can be maintained, although the detailed heat distribution may differ from the laboratory-scale configuration. However, because such limitations influence static and dynamically adapted operation in a comparable manner, the relative performance trends and the qualitative benefit of simplified dynamic control strategies are expected to remain robust when extrapolated to larger-scale DAC deployments.

3.6. Key performance indicators

To evaluate different process options for adsorption-based DAC, a set of Key Performance Indicators (KPIs) is required. These KPIs are derived from the simulation outputs of Aspen Adsorption. The specific electrical energy demand consists of the energy consumed by both the air fan (see Eq. (5)) and the vacuum pump (see Eq. (6)) per ton of CO_2 produced. The fan energy demand is calculated using a standard pressure drop correlation as implemented in Aspen Adsorption [40] while the vacuum pump energy demand is based on the assumption of isothermal compression and follows an expression adapted from Stampi-Bombelli et al. [11]. The total electrical energy demand is obtained by summing these two contributions and is defined in the present study (see Eq. (7)).

$$E_{Fan} = \frac{1}{m_{CO_2,produced}} \frac{\dot{V}_{Air}\Delta p}{\eta_{fan}} \left[\frac{MWh}{t_{CO_2}}\right] \tag{5}$$

$$E_{VP} = \frac{1}{m_{CO_2,produced}} \frac{\dot{n}RT}{\eta_{VP}} \ln\left(\frac{p_H}{p_L}\right) \left[\frac{MWh}{t_{CO_2}}\right] \tag{6}$$

$$E_{el} = E_{Fan} + E_{VP} \left[\frac{MWh}{t_{CO_2}}\right] \tag{7}$$

The specific thermal energy demand consists of the duty of the heat exchanger at the adsorption chamber and the produced mass of CO_2 (see Eq. (8)). This formulation is based on the resolved temperature gradient along the column and is also implemented in Aspen Adsorption [40].

$$E_{HEx} = E_{th} = \frac{1}{m_{CO_2,produced}} \dot{m}_{Flow} c_p \frac{dT_{HEx}}{dz} dz \left[\frac{MWh}{t_{CO_2}}\right] \tag{8}$$

The total specific energy demand is defined as the sum of thermal and electrical energy demands (see Eq. (9)).

$$E_{tot} = E_{th} + E_{el} \left[\frac{MWh}{t_{CO_2}}\right] \tag{9}$$

Finally, the CO_2 productivity is determined by dividing the produced

CO_2 mass by the duration of one cycle. (see Eq. (10)).

$$Pr = \frac{m_{CO_2\,produced}}{t_{Cycle}} \left[\frac{t_{CO_2}}{d}\right] \tag{10}$$

Both the definitions of total energy demand and productivity are introduced by the authors in this study. Further explanation of the employed terms, symbols and units can be found in Table 2 and the SI in section 1, Table 6.

3.7. Optimization parameter selection

Adsorption-based DAC systems are influenced by a large number of process parameters, including airflow rate, desorption conditions, and the durations of individual cycle steps. A structured sensitivity analysis is therefore necessary to determine which parameters are most relevant for optimization under weather-dependent operation. Here, we adopt insights from Zhang et al. [23], who performed a detailed parametric evaluation of TVSA desorption conditions, complemented by a preliminary sensitivity screening using the developed model.

Parameters that cannot be adjusted operationally, such as adsorber geometry and material properties, were excluded from dynamic optimization. This leaves seven variables that could theoretically be adapted during operation: adsorption air flowrate, desorption temperature, desorption pressure, and the durations of adsorption, evacuation, desorption, and cooling.

Consistent with Zhang et al. [23] and confirmed by our own preliminary screening simulations, thermal efficiency improves at higher desorption temperatures and lower desorption pressures due to increased driving force for regeneration. However, these trends lead to physically unrealistic extreme conditions when optimized solely for minimal specific energy demand and do not account for material stability limits, exergy losses, or industrial vacuum system constraints. Therefore, desorption temperature and pressure are held constant within realistic operating ranges and excluded from the optimization formulation. Similarly, the adsorption flowrate presents a trade-off between specific energy demand and productivity. Minimizing the specific energy demand alone would drive the flowrate to unrealistically low values, resulting in excessive cycle durations and high capital costs. Since productivity is handled separately in the techno-economic assessment, airflow is fixed in this study.

The evacuation and cooling steps exhibit limited influence on energy demand in our screening and contribute minimally to cycle time relative to adsorption and desorption. Additionally, no heat integration measures are considered during cooling. These steps are therefore not included in the optimization. An overview of the fixed parameters is shown in Table 3.

As a result, adsorption duration and desorption duration are selected as the key dynamically adjustable variables for optimization in response to weather variability. This focused scope enables a computationally efficient yet physically meaningful evaluation of dynamic operation strategies.

The adsorption time is influenced by weather conditions, as these determine the adsorption equilibrium and thus the time required to achieve a target CO_2 loading. The desorption time, in contrast, is governed by both the adsorption and desorption equilibrium, making its optimization equally relevant. To prevent unrealistic desorption times driven by the purely energy-minimizing objective and the adiabatic assumption in the model, an operational cut-off criterion is defined for terminating the desorption step. The cut-off is based on the residual CO_2 loading inside the adsorbent. Specifically, the desorption step ends once the molar flow of CO_2 in the product stream falls below 1e-6 mol s^{-1}. Sensitivity checks showed that this threshold corresponds to a final solid-phase loading of approximately 5–10 % of the minimum achievable loading at the given desorption conditions, i.e., a regeneration degree of about 90–95 %. Below this point, the desorption becomes increasingly slow, and further CO_2 removal yields diminishing energetic benefit. This stopping condition therefore ensures that the optimization explores only technically meaningful desorption durations while still capturing the dominant regeneration behavior relevant to practical DAC operation.

3.8. Process optimization

To enable automated parametric studies and optimization, the simulation was coupled to MATLAB R2024a [45] following the approach of Hamedi et al. [46]. This setup establishes a live connection between MATLAB and Aspen Adsorption, allowing MATLAB to start, stop, reset, and manipulate the simulation by adjusting defined input parameters. Output variables are extracted after each run, making it possible to implement an automated optimization loop that significantly reduces manual workload and enables systematic analysis of varying ambient and operational conditions. The employed MATLAB scripts are provided in section 4.3 in the SI.

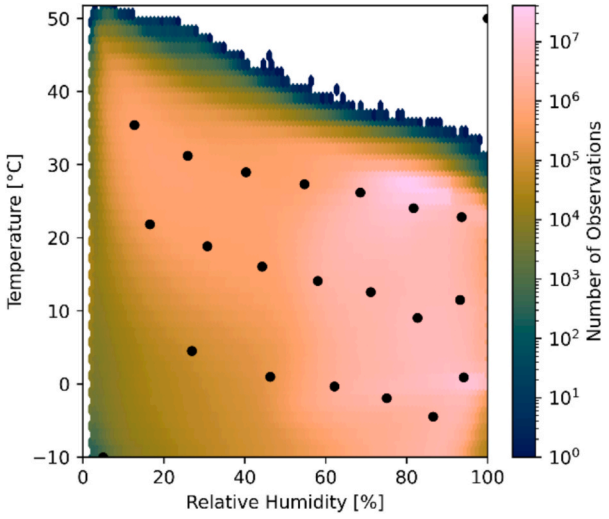

Fig. 2. Temperature and relative humidity clusters derived from an analysis of hourly-resolved weather data.

Table 6
Comparison of static and dynamic process operation of TVSA-based DAC process. The regions correspond to the first administrative level in each country, e.g., federal states. USA.19_1 is Louisiana, DEU.8_1 is Mecklenburg-Vorpommern, NGA.3_1 is Akwa Ibom and NOR.10_1 is Nordland.

	Static operation		Dynamic operation		Energy savings	
	E_{th}	E_{el}	E_{th}	E_{el}	Thermal	Electrical
	MWh/t_{CO2}	MWh/t_{CO2}	MWh/t_{CO2}	MWh/t_{CO2}	%	%
NGA.3_1	3.835	0.817	3.818	0.760	0.443	6.977
NOR.10_1	3.228	0.613	3.211	0.559	0.527	8.809
USA.19_1	3.316	0.690	3.301	0.650	0.452	5.797
DEU.8_1	3.243	0.639	3.214	0.590	0.894	7.668

3.8.1. Optimization loops

The optimization was conducted for a total of 22 temperature and relative humidity (T-RH) combinations (see Fig. 2). Twenty of these combinations are obtained from a probabilistic analysis of globally distributed, hourly weather data for the year 2018, resolved at a spatial resolution of 0.25° x 0.25° [47]. The dataset was clustered using a k-means algorithm, and the resulting combinations correspond to the respective cluster centers (see section 3.3 in the SI). For this study, temperatures below − 10 °C are excluded as the employed thermodynamic model is not validated for this temperature range. In addition to these twenty points, we add two points to the bottom-left and top-right sections of the diagram to include extreme conditions. All combinations are listed in Table 5.

The selection of representative ambient conditions was intended to ensure that the optimization outcomes reflect atmospheric states frequently encountered worldwide, thereby increasing the practical relevance of the findings for real TVSA operation. Since many locations transition between different T-RH combinations on daily or seasonal timescales, the process model is designed to dynamically adjust its operating point in response to such variability. This results in corresponding changes in adsorption and desorption durations to maintain energy-efficient operation under fluctuating climatic conditions.

For each optimization loop, the adsorption duration is varied across a predefined range. The simulation is initiated with an adsorption time of 25 min (20 min for clusters 10, 11, and 22) and subsequently increased in 1-minute increments up to 60 min. This yields 36 iterations per cluster (41 iterations for clusters 10, 11, and 22). For each iteration, the predefined KPIs are stored. After completion, the data is analyzed to identify the operating point yielding the lowest total specific energy demand (E_{tot}), which defines the optimal adsorption and desorption durations for the respective cluster.

The first cycle of each simulation primarily reflects the imposed initial conditions rather than weather-dependent behavior and is therefore excluded from evaluation. Cyclic steady state is reached after the second cycle. Consequently, three full cycles are simulated for each iteration, and only results from the final cycle are retained for further analysis.

3.8.2. Post-processing of the optimization data

While the optimization was initially performed for 22 representative T-RH clusters, real-world weather conditions vary continuously and do not necessarily coincide with the cluster centers. To ensure applicability across the full range of relevant atmospheric states, an extended simulation campaign was conducted. A total of 140 T-RH combinations were defined by discretizing the operating domain into increments of 10 °C (−10 °C to 50 °C) and 5 % RH (5 % to 100 %).

For each of the 22 optimized operating points (adsorption and desorption durations), the process model was simulated over all 140 T–RH combinations while keeping the cycle parameters fixed. This resulted in 22 datasets, hereafter referred to as screening plots, each describing the specific energy demand over the full climatic domain for a single operating strategy (see Fig. 3).

The optimal operating strategy for each T-RH combination was then determined by comparing the total specific energy demand across all screening plots and selecting the configuration with the lowest value. By assigning each T-RH condition to its most energy-efficient operating point, a final combined map, referred to as the comprised plot, was constructed. This plot consolidates performance data from all screening plots and indicates the most favorable operating strategy across the full climatic domain. In addition to total specific energy demand, all other KPIs were stored, enabling the construction of corresponding comprised plots for different performance metrics.

3.9. Techno-economic assessment

Utilizing the comprised KPIs, a techno-economic assessment (TEA) is conducted to evaluate the impact of weather conditions on DAC costs. The TEA considers four exemplary regions in the US (Louisiana), Germany (Mecklenburg-Vorpommern), Norway (Nordland), and Nigeria (Akwa Ibom). These are chosen to reflect a broad range of climatic conditions and to ensure relevance through available infrastructure. The inclusion of the US site is further supported by ongoing DAC project developments [48]. To incorporate the influence of weather conditions, the derived weather-dependent DAC KPIs are combined with hourly resolved weather data [47] to generate time series data for the specific energy demand and the relative productivity of DAC plants in each of the considered regions. The weather year 2018 has been selected for this assessment, as it represents an average year for renewable energy generation and is commonly used in global studies [49,50]. In the base scenario, the DAC model is combined with fixed energy costs of 80 €/MWh_{el} and 20 €/MWh_{th} and is designed to remove 50 t_{CO2} annually, reflecting the size of a prototype plant. Fixed energy costs were chosen in this assessment to highlight the impact weather exclusively has on the DAC plant without accounting for variable energy costs.

However, because DAC systems are typically powered by renewable energy sources, whose output is strongly influenced by weather conditions as well, an additional assessment was conducted in which open-field PV (OFPV) systems serve as the sole electricity supply. This is particularly relevant as the availability of low-cost renewable energy exerts a major influence on the levelized cost of DAC (LCOD) [35]. For this purpose, variable PV time series generated using the ETHOS.RESKit tool [51] and developed in coordination with the International Energy Agency for the Global Hydrogen Review 2024 [49] were employed in this study. Further details on the PV generation data can be found in the study of Winkler et al. [52]. The general workflow of the TEA is described in our previous work [35]. In the PV-only supply scenario, battery storage is included, and heat demand can be met either via heat pumps or electric heaters. The corresponding techno-economic parameters are summarized in Table 4.

The LCOD are derived using the ETHOS.FINE [55] framework which

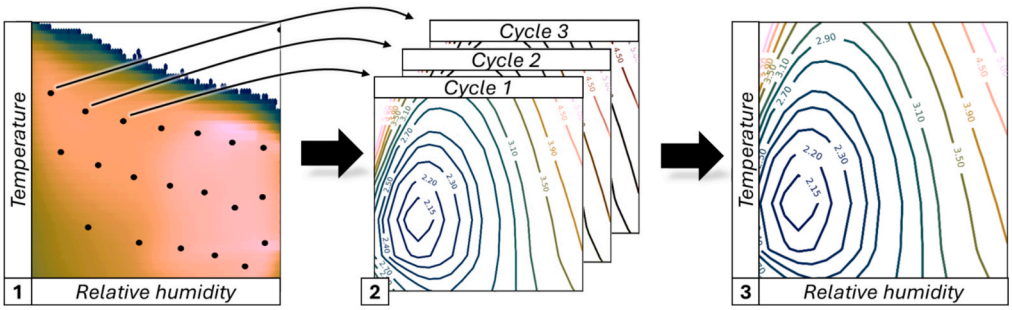

Fig. 3. Visualization of the processing of the optimization data with (1) showing the derivation of 22 most probable weather clusters, (2) showing the 22 optimal adsorption cycles and the resulting screening plots with KPI data for all 140 T-RH combinations and (3) showing the comprised plot including data from all 22 screening plots maintaining minimal specific energy demand for every T-RH combination.

optimizes both plant capacity and hourly operation to minimize the total annual system cost. Given that this study focuses on a prototype system and aims to explore the influence of the environmental conditions, higher capital expenditures (CAPEX) have been chosen, which are more likely to represent today's system costs. In the base scenario the CAPEX for the DAC plant are assumed to be 3000 €/(t_{CO2}/a), based on [56], with fixed annual operational expenditures (OPEX) set at 4 % of the CAPEX [57]. The economic lifetime of the system is set at 20 years, with a discount rate of 7 % [57]. All currency values are stated in 2024 €. The structure of the techno-economic assessment is visualized in Fig. 4.

4. Results and discussion

4.1. Process optimization results

The results of the optimization procedure for each weather combination are summarized in Table 5. The optimal adsorption durations range from 24 to 42 min, while optimal desorption durations vary between 58 and 83.5 min. These findings demonstrate that ambient conditions strongly influence the required cycle configuration to maintain optimal operation. In particular, operation under highly humid conditions (>80 %) necessitates extended desorption durations. Nevertheless, even with optimized cycle times, the specific energy demand of the process remains sensitive to ambient conditions. A detailed assessment of the energy demand is provided in the following sections.

4.2. Process analysis and derived KPIs

The contour plots shown in Fig. 5 illustrate the optimized thermal and electrical specific energy demand as a function of ambient temperature and relative humidity under optimal operation. To fully understand the observed trends, it is important to consider the influences of the total energy input (numerator) and the amount of CO_2 captured (denominator) on the specific energy demand.

A minimum in specific energy demand (2.57 MWh/t_{CO2}) is observed at approximately 10 °C and 25 % RH in both plots. Under these conditions, the developed TVSA process operates with the highest energy efficiency, making them the most favorable climatic conditions for DAC operation. Away from this optimal operation, the specific energy demand increases in all directions due to competing effects of adsorption capacity and energy consumption.

At lower temperatures, the CO_2 adsorption capacity of the adsorbent increases, which also increases the amount of CO_2 that can be captured per cycle. However, this benefit is offset by an increase in thermal energy demand due to the higher energy required to heat the adsorption chamber during desorption. Consequently, the specific energy demand rises at very low temperatures. At higher temperatures, the opposite trend is observed. The total energy input decreases since less heat is required to reach desorption temperatures, but the CO_2 adsorption capacity declines, leading to a decreased CO_2 output. As a result, the specific energy demand increases, despite the lower absolute energy input.

At low humidity levels (<20 % relative humidity), less water is adsorbed (see Fig. 8) and the beneficial co-adsorption effect of water is weakened, reducing CO_2 adsorption capacity and therefore increasing the specific energy demand. The lower overall CO_2 uptake leads to a lower denominator in the specific energy equation, increasing its value. At higher humidity levels, more water adsorbs, and CO_2 adsorption is increased due to the co-adsorption effect. However, this enhancement is counteracted by the increased energy demand needed to evaporate and remove the co-adsorbed water during desorption. This additional energy input increases the overall specific energy demand in humid conditions. This effect is especially prominent at higher temperatures (>30 °C) and higher relative humidities (> 90 %).

For validation, the predicted energy demand trends were compared to the contour results derived from data reported by Sendi et al. [17], who evaluated a weather-dependent DAC process using the same adsorbent material. As shown in Fig. 6 and Fig. 7, both studies exhibit consistent qualitative sensitivities with respect to temperature and humidity. Minor quantitative deviations are expected due to the different desorption heat supply (TVSA vs. S-TVSA) and optimization objectives. Importantly, the location and magnitude of the optimal operating region (≈10–15 °C and 20–30 % RH) are closely aligned. This agreement confirms that the developed model reliably captures the climatic performance trends of amine-based DAC systems.

Sendi et al. present even lower and narrower energy demand values (1.5–4 MWh/t_{CO2}), which can be attributed to their use of a S-TVSA process [17]. Steam reduces the CO_2 partial pressure during desorption, enhancing working capacity and reducing energy input. In our study, a dry TVSA process was selected to avoid additional complexity related to steam–adsorbent interactions. As a result, the effect of warm and dry ambient conditions is more pronounced in our simulations: the specific energy demand increases drastically as temperature further increases and humidity decreases. This behavior is driven by the low CO_2 production rates shown in Fig. 5. Elevated temperatures and the absence of co-adsorbed water reduce CO_2 uptake, leading to the lowest CO_2 productivity at 50 °C and 5 % RH. To operate a TVSA DAC process under such conditions, more stringent desorption conditions, i.e., lower vacuum pressures and/or higher desorption temperatures, are required to achieve sufficient CO_2 working capacity. Alternatively, a S-TVSA process may be employed.

Wiegner et al., who optimized for productivity rather than energy efficiency and used a different adsorbent material, report overall specific energy demands between 1 and 9 MWh/t_{CO2} with a dominant dependence on temperature and little influence of relative humidity, except under very dry or very humid conditions [18]. In contrast, results of this

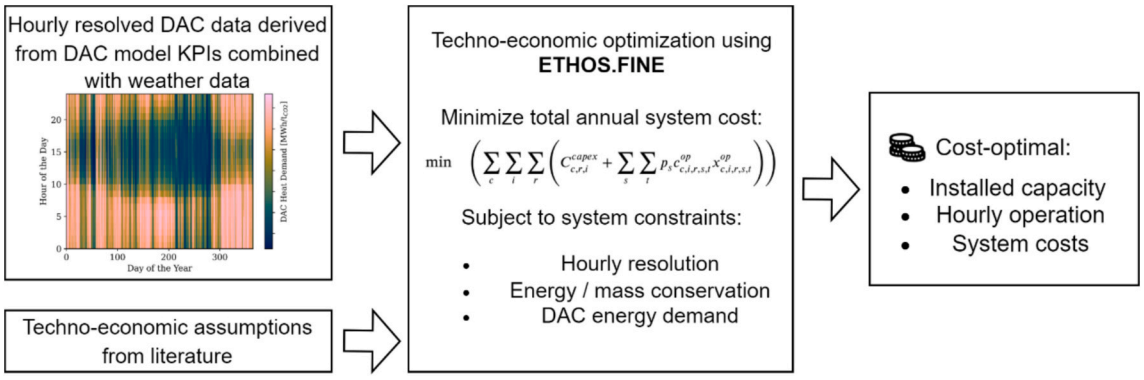

Fig. 4. Structure of the techno-economic assessment highlighting the input data as well as the resulting outputs. The ETHOS.FINE framework is utilized for the optimization [55,58] and all assumptions are stated in the previous chapter.

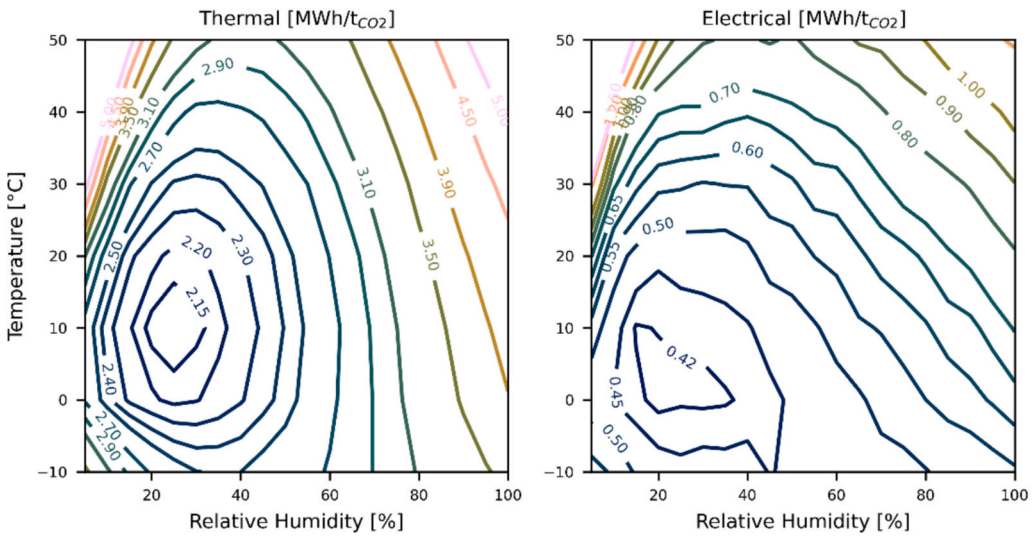

Fig. 5. Comprised plot of the specific thermal and electrical energy demand considering optimized operation mode.

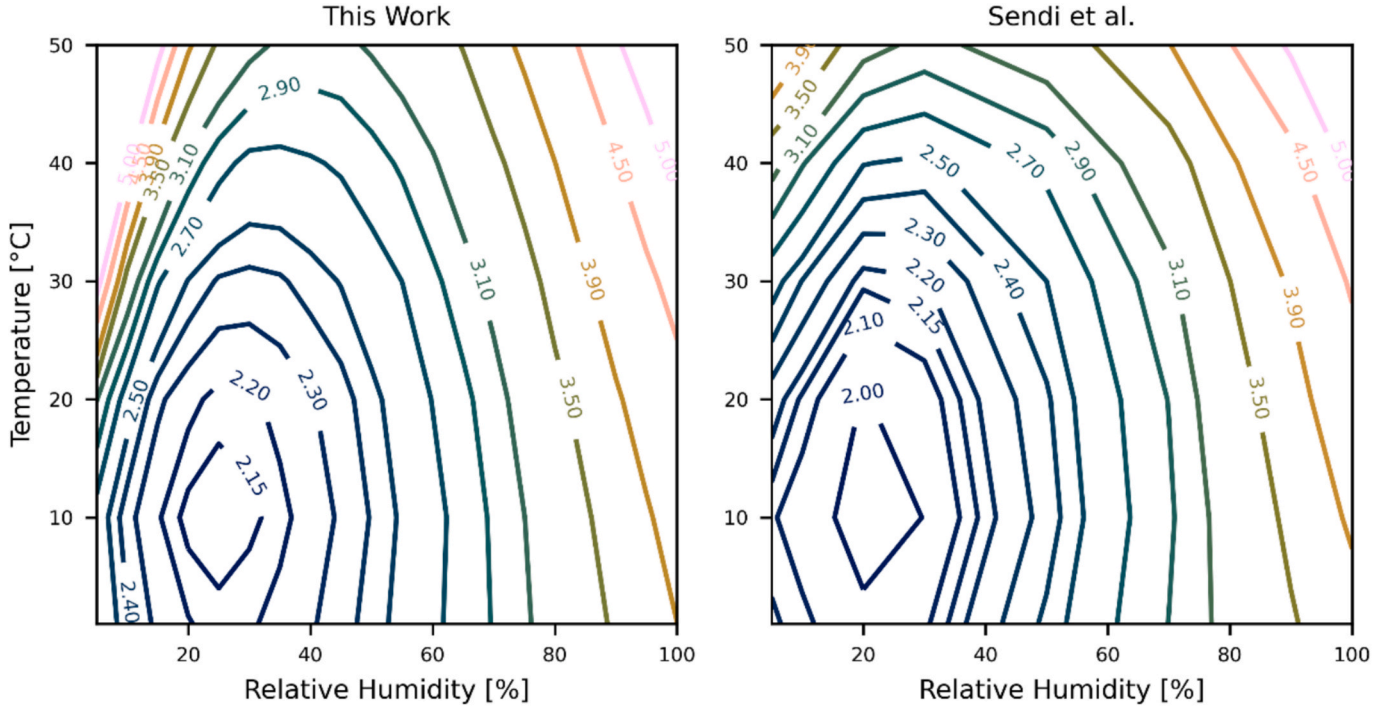

Fig. 6. Comparison of the specific thermal energy demand of this work and the study of Sendi at al.

study show a stronger and more consistent effect of humidity, particularly between 0–20 °C and 50–75 % RH, where temperature has little impact, but humidity significantly affects thermal energy demand. The absence of a co-adsorption model in the study by Wiegner et al. leads to an underestimation of humidity effects. Additional discrepancies are rooted in different optimization objectives and modeling assumptions.

Fig. 8 presents the relative productivity (A) and the water co-adsorption ratio (B) of the optimized operating points as a function of ambient temperature and relative humidity. The relative productivity is defined as the ratio of the CO_2 productivity of a given optimized operating point to the reference productivity at Cluster 1 (20 °C and 50 % RH), which is 0.0595 kg_{CO2}/day.

A maximum in productivity is observed at approximately 5 °C and 70 % RH. This peak can be attributed to the favorable CO_2 adsorption conditions at low temperatures and high humidity, which enhance the adsorption capacity of the employed adsorbent material. However, a decline in productivity is observed at very high humidity levels. While moderate humidity levels enhance CO_2 adsorption, excessive moisture can lead to excessive water adsorption, which must later be desorbed, thereby reducing the overall CO_2 productivity of the process. This is consistent with the trends seen in the specific energy demand (see Fig. 5), where high-humidity conditions require additional thermal energy input for water removal.

Nonetheless, the co-adsorbed water should not solely be viewed as an energetic burden. In arid regions, the water recovered during desorption may represent a valuable by-product of DAC operation. This water could be reused on-site, for example in downstream CO_2 conversion processes [59,60] or for conditioning geological sequestration streams [61,62], potentially improving the overall economic viability of the plant. To date, temperature- and humidity-dependent water co-adsorption data

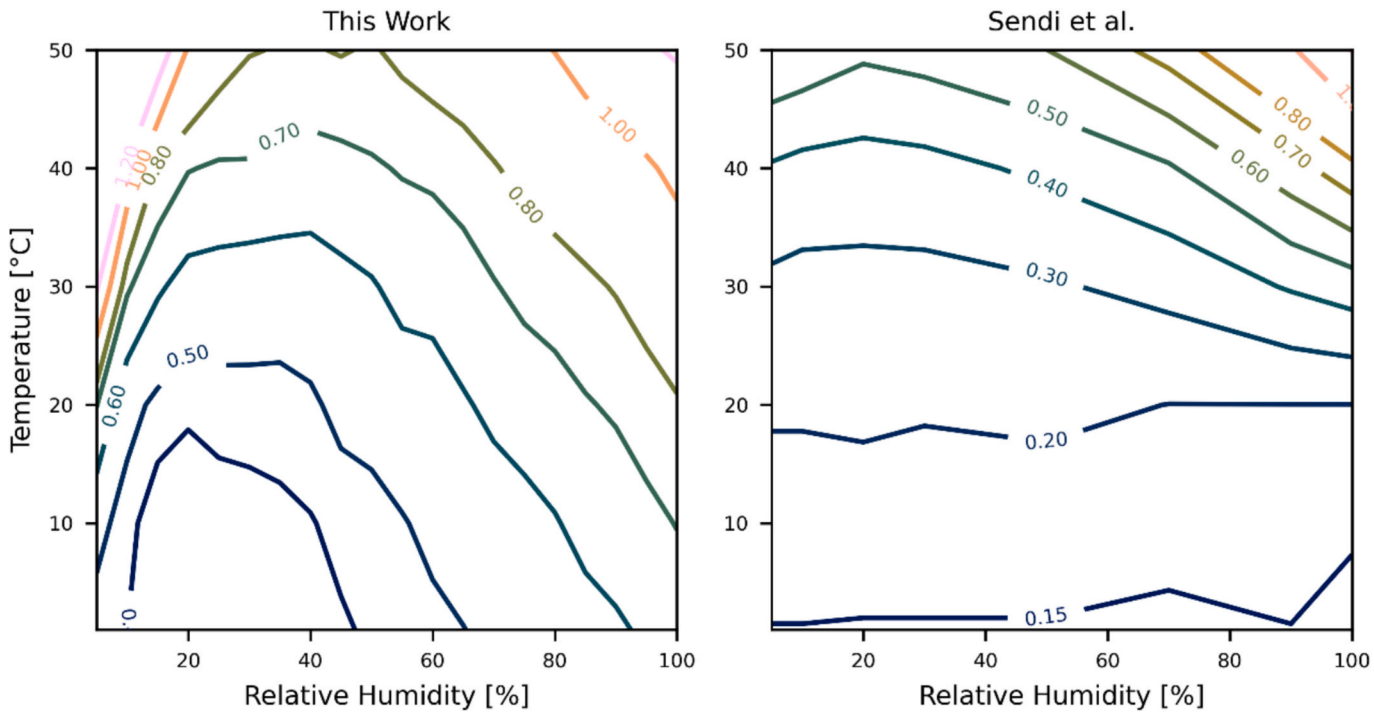

Fig. 7. Comparison of the specific electrical energy demand of this work and the study of Sendi at al.

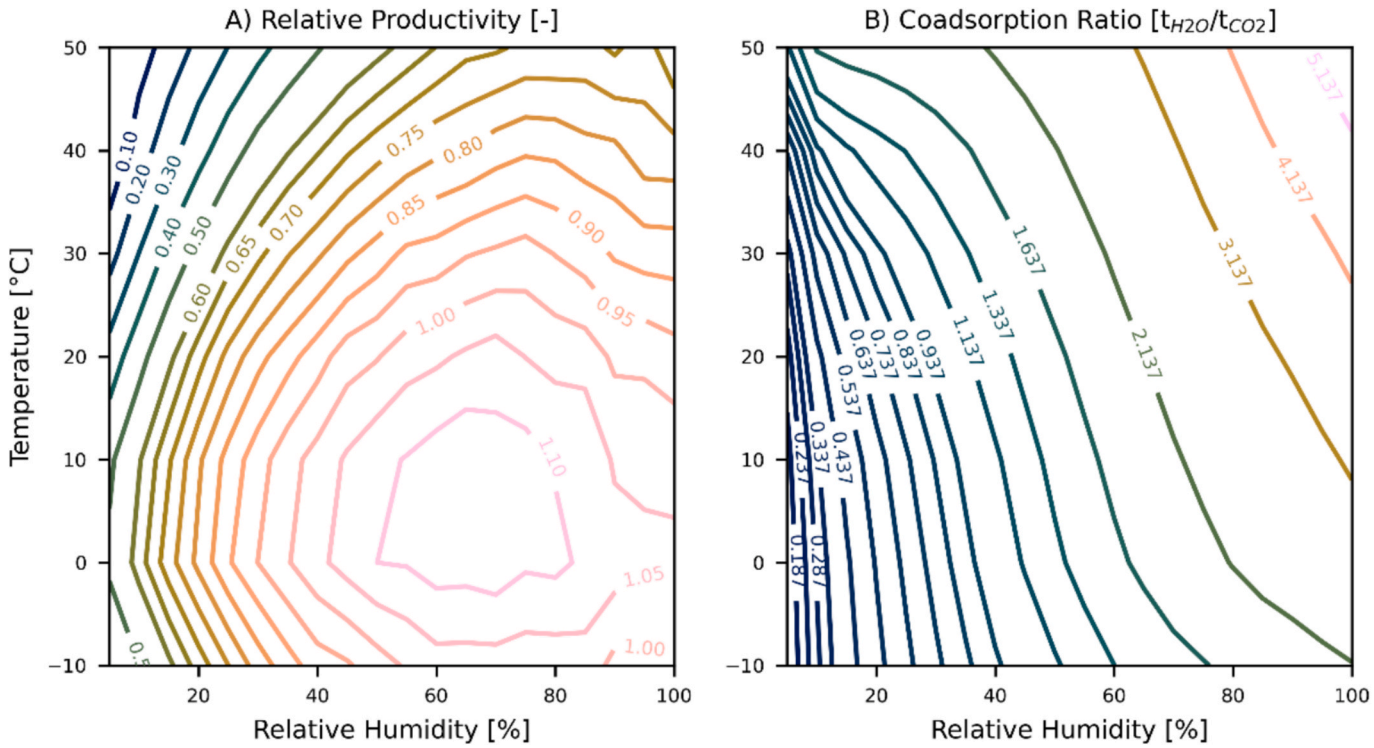

Fig. 8. Influence of weather on relative productivity (A) and water co-adsorption ratio (B).

are only sparsely reported in literature. Therefore, the results presented in Fig. 8(B) offer a valuable foundation for further analyses on integrated water and carbon recovery from ambient air.

The identified productivity trends (see Fig. 8(A)) partly align with the findings of both Sendi et al. [17] and Wiegner et al. [18], who also report maximum CO_2 productivity under cold and moderately humid ambient conditions. In all three studies, such conditions are associated with enhanced CO_2 adsorption capacity and favorable process performance. In the present study, a nonlinear interaction between ambient temperature and relative humidity is observed. Sendi et al. [17], report similar productivity trends to those found here, likely due to the use of the same adsorbent material. In addition, the present study considers a broader range of ambient conditions (−10 °C to 50 °C and 5 % to 100 % RH) and applies a high-resolution parametric analysis over 140 distinct

operating points. In contrast, the results presented by Wiegner et al. [18] suggest that productivity is predominantly influenced by temperature, with a comparatively limited sensitivity to humidity. Again, this is consistent with the fact that their model does not include an explicit co-adsorption formulation, which is expected to lead to an underestimation of humidity effects.

In summary, the analysis confirms that moderate ambient temperatures and relative humidity levels lead to the most favorable performance of a TVSA-based DAC process, both in terms of specific energy demand and CO_2-productivity. These dependencies are primarily driven by the thermodynamic effects of CO_2-H_2O co-adsorption, which significantly influence working capacity and energy requirements. The results underline the importance of considering local climate conditions and detailed co-adsorption behavior in the design and operation of DAC systems.

4.3. Process-informed evaluation of a dynamic operation strategies for DAC systems

To evaluate the potential benefits of a dynamic operating strategy, a hypothetical DAC plant is simulated under hourly-resolved weather conditions at four different locations in: Nigeria, Norway, the US, and Germany. Details of the weather data are provided in section 3.3 in the SI. The aim of the dynamic operation is to continuously adjust relevant process parameters in response to ambient temperature and relative humidity, thereby maintaining an optimal operating point on an hourly basis.

For the static operating strategy, a single set of process conditions, i.e., fixed adsorption and desorption durations, is applied throughout the entire year. In this case, the process configuration of cluster 1 is chosen (see Table 5). In contrast, the dynamic operation strategy employs the comprised plot, i.e., the optimal cluster in each operation point (see Fig. 5). For both strategies, the hourly energy demand is determined and subsequently averaged over the full year to derive the annual mean specific energy demand for each location. This enables a quantitative comparison of the specific energy requirements associated with static versus dynamic operation.

Additionally, two further strategies are evaluated: Day-night cycles as well as seasonal cycles. For the day-night strategy, the DAC plant adjusts its process parameters twice per day, at 8 am for the day cycle and at 8 pm for the night cycle. To determine the corresponding operating conditions, the average weather parameters for daytime (8 am to 7 pm) and nighttime (8 pm to 7 am) are computed, and the nearest cluster is selected as the operating state. This approach could be implemented in practice using short-term weather forecasts and requires less control effort than hourly adaptation. The third adaptation strategy applies seasonal cycles, in which operating conditions are adjusted only twice per year – once for summer (April to September) and once for winter (October to March) – based on the average weather conditions of each season.

The results of the static and dynamic operation comparison across the different locations are summarized in Table 6, while Table 7 shows the results of the day-night cycle strategy and Table 8 highlights the results of the seasonal cycles. The potential thermal energy savings are highest for the hourly adjusted dynamic operation, ranging from 0.443 % in Nigeria to 0.894 % in Germany. In contrast, the electrical energy savings are larger, varying between 5.797 % (United States) and 8.809 % (Norway). These findings indicate that dynamic operation primarily influences electrical energy consumption, whereas the reduction in thermal energy demand remains comparatively minor across all locations. Despite the relatively large percentage reduction in electrical energy demand, its contribution to the total energy balance remains smaller than that of thermal energy. As a result, the maximum total energy savings, observed in Germany, reach only approximately 2 %. This indicates that the advantages of dynamically adjusting operating conditions in response to hourly weather fluctuations are relatively limited. Considering these modest benefits, together with the requirement for a more sophisticated control strategy, it appears unlikely that fully dynamic operation would be economically or practically justified in most applications.

However, the results for the day–night and seasonal cycles demonstrate that less frequent adjustments of the operating conditions can achieve savings comparable to those of fully dynamic operation. In particular, the electricity savings obtained with the day–night strategy are similar to those reached under hourly dynamic operation (cf. Table 6), indicating that meaningful improvements can be realized without the need for continuously adjusted operating parameters. Moreover, the seasonally adjusted strategy, where operational parameters are updated only twice per year, also exhibits noteworthy potential for energy savings. These findings suggest that an optimized selection of operating cycles, tailored to regional climate characteristics, can yield relevant energy reductions. At the same time, they indicate that highly sophisticated strategies requiring continuous, weather-driven adjustments are neither necessary nor likely to be economically feasible.

Table 7
Energy demand of the day-night cycle operation strategy as well as energy savings compared to static operation.

	Day-Night Cycles		Energy Savings	
	E_{th}	E_{el}	Thermal	Electrical
	MWh/t_{CO2}	MWh/t_{CO2}	%	%
NGA.3_1	3.820	0.761	0.391	6.854
NOR.10_1	3.214	0.559	0.434	8.809
USA.19_1	3.302	0.656	0.422	4.928
DEU.8_1	3.216	0.592	0.833	7.355

Table 8
Energy demand of the seasonal cycle operation strategy as well as energy savings compared to static operation.

	Seasonal Cycles		Energy savings	
	E_{th}	E_{el}	Thermal	Electrical
	MWh/t_{CO2}	MWh/t_{CO2}	%	%
NGA.3_1	3.820	0.776	0.391	5.018
NOR.10_1	3.220	0.560	0.248	8.646
USA.19_1	3.309	0.671	0.211	2.754
DEU.8_1	3.224	0.596	0.586	6.729

4.4. Techno-economic assessment

The results of the TEA are presented in Table 9. It is evident that LCOD are significantly influenced by regional weather conditions, with values ranging from 496 €/t_{CO2} in Germany to 568 €/t_{CO2} in Nigeria. Given that fixed energy costs were assumed across all regions in the base

Table 9
Results of the techno-economic assessment for the four regions considered. The regions correspond to the first administrative level in each country, e.g., federal states. USA.19_1 is Louisiana, DEU.8_1 is Mecklenburg-Vorpommern, NGA.3_1 is Akwa Ibom and NOR.10_1 is Nordland.

	USA.19_1	DEU.8_1	NGA.3_1	NOR.10_1
LCOD [€/t_{CO2}]	523	496	568	517
Installed Nominal DAC Capacity [t_{CO2}/a]	50.2	47.7	53.3	50.5
Average Electricity Demand [MWh_{el}/t_{CO2}]	0.72	0.67	0.85	0.64
Average Heat Demand [MWh_{th}/t_{CO2}]	3.38	3.31	4.00	3.31
Average Water Co-Adsorption [t_{H2O}/t_{CO2}]	2.74	2.49	3.59	2.34
Average Relative Productivity [-]	1.03	1.09	0.99	1.03

scenario, these variations arise solely from differences in energy demand and relative productivity, both of which are imposed by local weather conditions. For instance, the average specific electricity demand is 0.67 MWh_{el}/t_{CO2} in Germany while it is 0.85 MWh_{el}/t_{CO2} in Nigeria. This discrepancy is attributed to Nigeria's hotter and more humid climate, which creates less favorable operating conditions for DAC (see Fig. 5). However, the difference in energy demand alone does not fully explain the observed cost variation. When comparing Germany and Nigeria, the increased energy demand accounts for only 28 €/t_{CO2} of the cost difference. The remaining discrepancy arises from differences in relative productivity, which directly influence the required nominal DAC capacity. Specifically, in Germany, 5.6 t_{CO2}/a less nominal capacity is required compared to Nigeria, leading to reduced capital cost and fixed OPEX in total contributing 45 €/t_{CO2} in cost savings. These findings highlight that relative productivity is the primary driver of regional LCOD variations for adsorption-based DAC. Consequently, solid sorbent DAC deployment should be prioritized in regions characterized by lower temperatures and moderate relative humidity, as these conditions enhance productivity and reduce costs (see Fig. 8). Additionally, lower specific energy demand is generally found in these regions.

To assess the impact of the different parameters on the LCOD, a sensitivity analysis was conducted. CAPEX, levelized cost of electricity (LCOE), and levelized cost of heat (LCOH) were varied by ± 50 %, evaluating their influence on LCOD across all four regions. The results of this sensitivity analysis are presented in Fig. 9.

The results indicate that specific CAPEX have the most substantial impact on LCOD. The magnitude of this effect varies by region, with Nigeria exhibiting the highest sensitivity, where LCOD changes by ± 215 €/t_{CO2}, while Germany experiences the lowest variation at ± 192 €/t_{CO2}. This discrepancy is explained by Germany's higher relative productivity, which reduces the required nominal DAC capacity and, consequently, reduces the influence of CAPEX fluctuations on overall costs. In contrast, variations in the LCOH and LCOE have a comparatively small impact on LCOD. In the US, for instance, changes in LCOH and LCOE result in cost variations of ± 33 €/t_{CO2} and ± 26 €/t_{CO2}, respectively. Although LCOH are significantly lower than LCOE, changes in LCOH exert a greater influence due to the higher quantity of heat required for DAC operation. This analysis underscores the significant role of weather conditions in determining CO_2 removal costs via DAC, primarily due to their impact on plant productivity. In regions with lower productivity, larger DAC systems are required to achieve the same CO_2 removal targets, leading to increased costs. While CAPEX remain the dominant cost driver, regional energy demand is also a non-negligible factor. This effect is expected to become even more pronounced when DAC plants are integrated into renewable-based energy systems, where the variability of energy supply intersects with the time-dependent energy demand of DAC operations.

To evaluate the influence of variable renewable energy supply, an additional TEA is conducted in which power is exclusively supplied by OFPV panels. The resulting LCOD as well as the installed DAC, OFPV and battery capacities are detailed in Table 10. Compared with the scenario employing fixed energy prices and a constant energy supply, the LCOD increase substantially, reaching values between approximately 1000 and 1500 €/t_{CO2}. Across all regions, the energy system – comprising OFPV, batteries, heat pumps, and electric heaters – accounts for roughly half of the total cost, while the remaining half is attributed to the DAC plant itself. This underscores the significant cost implications associated with the intermittency of renewable energy. The primary reason lies in the high CAPEX of the DAC unit, which requires high utilization to achieve low LCOD. Maintaining such utilization under variable PV supply necessitates substantial battery storage to bridge periods of low or absent generation. Moreover, larger DAC system capacities emerge as part of a trade-off between the cost of oversizing the DAC unit and the cost of building a more extensive energy supply system. The availability of favorable PV conditions constitutes an additional cost driver. This becomes evident when comparing the required OFPV capacities: in

Table 10
Results of the TEA based on power supply from OFPV.

	USA.19_1	DEU.8_1	NGA.3_1	NOR.10_1
LCOD [€/t_{CO2}]	998	1192	1108	1501
Installed Nominal DAC Capacity [t_{CO2}/a]	62	75.6	60.4	94.1
Installed OFPV Capacity [kW]	87.1	112.1	116	160.3
Installed Battery Capacity [kWh]	217.8	223.4	257.8	233.9

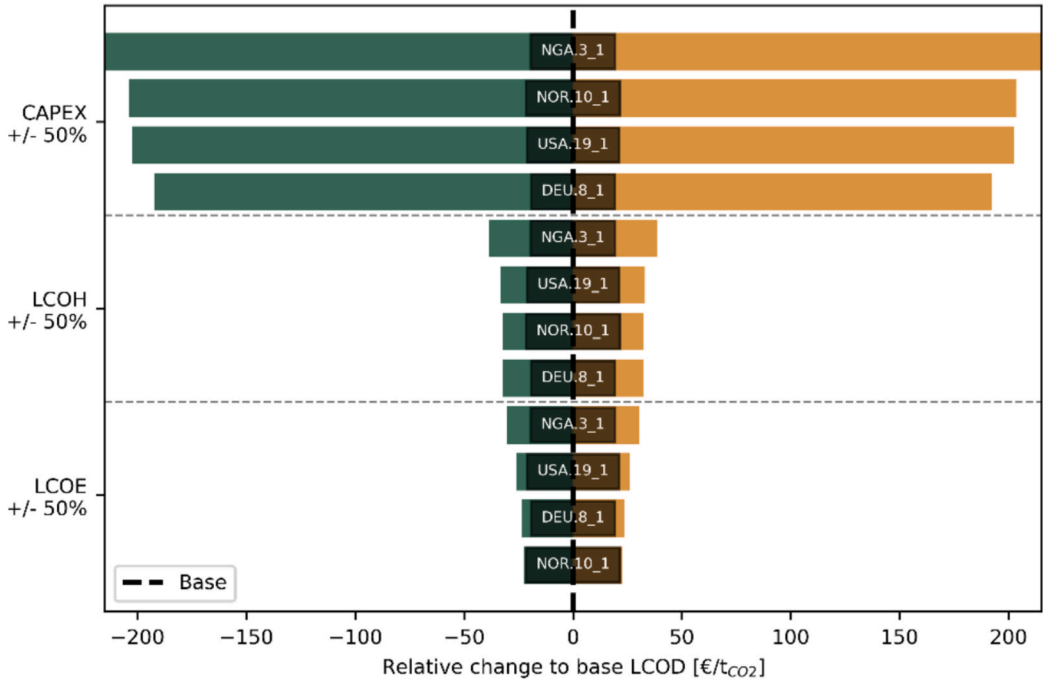

Fig. 9. Evaluation of the sensitivity analysis performed for four different regions.

northern Norway, the installed PV capacity is nearly twice that required in the southern United States, resulting in correspondingly higher system costs.

Since CAPEX of the DAC unit were identified as the dominant factor in the base scenario, the sensitivity analysis and the assessment of the PV-coupled system, an additional analysis was conducted to evaluate LCOD values across varying CAPEX levels, geographic regions, and energy cost scenarios. The results are compared to CAPEX projections reported in the literature [31]. The results are visualized in Fig. 10. It is evident that long-term CAPEX projections can result in different LCOD spanning a range of approximately 90 to 300 €/t_{CO2} depending on the energy cost and region. While future LCOD below 200 €/t_{CO2} are likely, LCOD of less than 100 €/t_{CO2} would require either extremely low energy cost or significant advances in DAC technology to lower energy requirements. At lower CAPEX, energy demand and cost dominate the resulting LCOD and oversizing of the DAC unit to shift DAC operation to times of lower energy demand becomes economically feasible. However, these effects are only observed at CAPEX below 300 €/(t_{CO2}/a) (see SI, Fig. 1).

5. Conclusion and outlook

5.1. Key findings

This study presents a detailed TVSA DAC process model that integrates an experimentally validated co-adsorption model for a commercially available sorbent with real-world weather data. The analysis reveals a strong dependence of DAC performance on ambient temperature and humidity, with optimal operation observed around 10 °C and 25 % RH. Both specific energy demand and CO_2 productivity exhibit non-linear variations with climatic conditions, reflecting the competing influences of co-adsorption enhancement and thermal regeneration requirements.

To evaluate the potential energy savings from dynamically adjusting operating conditions (e.g., cycle times), different operation strategies were compared. Fully dynamic operation can reduce the total specific energy demand by up to ~ 2 %, primarily through reductions in electrical energy consumption (5.8 to 8.8 %). Notably, most of these savings can be achieved using simplified strategies, such as seasonal or day–night adjustments, which realize similar performance gains to fully dynamic hourly control. These findings indicate that weather-adaptive operation is advantageous, but continuous real-time adjustments are not necessary to unlock most of the potential improvements.

Integrating the results of the developed process model into a techno-economic assessment indicates that productivity is the primary driver of capture costs, reflecting the strong impact of capital expenditures. Achieving LCOD values below 200 €/t_{CO2} appears realistic in future deployments, whereas reaching values below 100 €/t_{CO2} will likely require substantial process improvements or access to very low-cost electricity and heat.

5.2. Limitations

Several simplifying assumptions guide the interpretation of the absolute values. The adsorption column was modeled under adiabatic conditions with constant thermal properties, while real systems may exhibit some heat losses and non-uniform heat transfer. Intraparticle mass transfer was described using an LDF formulation, which captures overall kinetics but does not explicitly resolve pore-scale diffusion of CO_2 and H_2O. The reactor geometry reflects a laboratory-scale design; scaling to larger systems may introduce radial gradients, changes in pressure drop, or different heat-exchange configurations. Finally, dynamic operation was assumed to be adjustable at an hourly resolution, a scenario more readily applicable to stand-alone units than to modular systems with staggered cycles.

5.3. Implications and future work

From an operational perspective, the limited total-energy savings achieved by fully dynamic operation suggest that simplified adaptive strategies, such as seasonal or day–night switching, may provide a favorable balance between performance gains and control complexity. This has practical significance for early deployments where operational robustness and cost control are priorities. For policymakers and project developers, the results emphasize the importance of selecting deployment regions with favorable climate conditions and focusing innovative efforts on improving sorbent productivity and reducing capital costs. Future research should incorporate non-adiabatic column behavior, scale-dependent design features such as internal heat exchange, and further dynamic interactions with intermittent renewable energy systems. Although the present study focused on dynamic operation strategies aimed at reducing energy demand, expanding the objective function to jointly consider productivity and techno-economics may yield operating strategies better aligned with deployment needs. While this was beyond the scope of the current work, the integrated modeling framework developed here provides a foundation for such analyses and supports the advancement of weather-adapted DAC operation across diverse global locations.

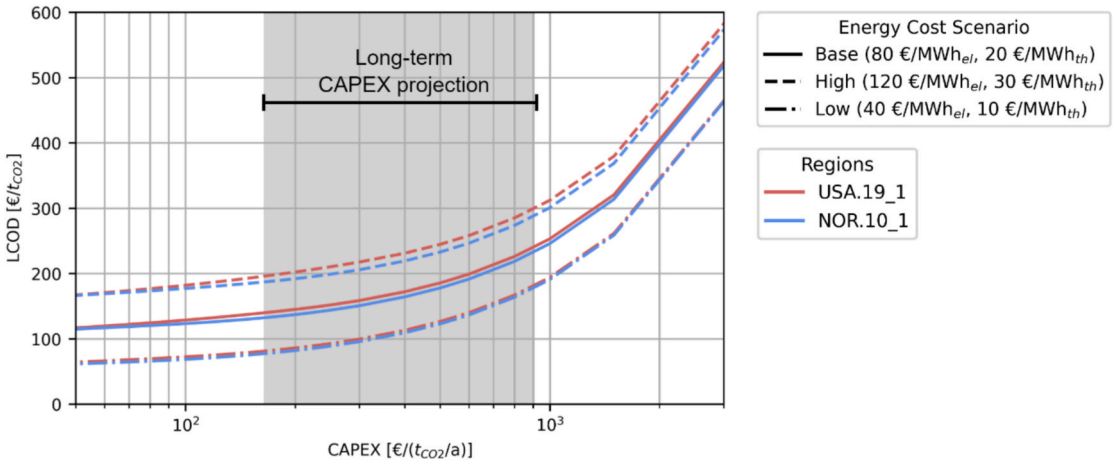

Fig. 10. Detailed analysis of the CAPEX variation and the resulting LCOD under different energy cost assumptions. The indicated grey area corresponds to long-term CAPEX estimations from a previous literature review [31].

6. Declaration of generative AI and AI-assisted technologies in the manuscript preparation process

During the preparation of this work the author(s) used ChatGPT and DeepL in order to improve the language of the manuscript. After using this tool/service, the author(s) reviewed and edited the content as needed and take(s) full responsibility for the content of the published article.

CRediT authorship contribution statement

Aaron S. Jajjawi: Writing – original draft, Visualization, Software, Methodology, Formal analysis, Conceptualization. **Henrik Wenzel:** Writing – original draft, Visualization, Methodology, Formal analysis, Conceptualization. **Freia Harzendorf:** Writing – review & editing, Supervision, Project administration. **Jann M. Weinand:** Writing – review & editing, Supervision. **Detlef Stolten:** Supervision, Project administration. **Ralf Peters:** Writing – review & editing, Supervision, Project administration.

Declaration of competing interest

The authors declare that they have no known competing financial interests or personal relationships that could have appeared to influence the work reported in this paper.

Acknowledgements

This work was performed as part of the project 'A Comprehensive Approach to Harnessing the Innovation Potential of Direct Air Capture and Storage for Reaching CO_2-Neutrality' (DACStorE), which is funded by the Initiative and Networking Fund of the Helmholtz Association (grant agreement number KA2-HSC-12).

Appendix A. Supplementary material

Supplementary data to this article can be found online at https://doi.org/10.1016/j.enconman.2025.121003.

Data availability

Data will be made available on request.

References

[1] IPCC, *Summary for Policymakers*, in *Climate Change 2023: Synthesis Report*, H. Lee, Romero, J., Editor. 2023, IPCC: Geneva, Switzerland. p. 1-34.
[2] Abbasi S, Ahmadi Choukolaei H. A systematic review of green supply chain network design literature focusing on carbon policy. Decis Anal J 2023;6.
[3] Edelenbosch OY, et al. Reducing sectoral hard-to-abate emissions to limit reliance on carbon dioxide removal. Nat Clim Chang 2024;14(7):715–22.
[4] Zanobetti F, Dal Pozzo A, Cozzani V. Sustainability assessment of CO_2 capture across different scales of hard-to-abate emission sources. Chem Eng J 2025;505.
[5] Abbasi S, et al. Using a just-in-time approach in the green supply chain, taking into account CO_2 emissions, under uncertainty in the pre- and post-COVID-19 situation. Discret Dyn Nat Soc 2025;2025(1).
[6] Ozkan M, et al. Current status and pillars of direct air capture technologies. iScience 2022;25(4).
[7] Buckett, A. *Mammoth undertaking: Climeworks starts up world's largest direct air capture plant*. 2024 10.05.2024 [cited 2025 14.03.]; Available from: https://www.thechemicalengineer.com/news/mammoth-undertaking-climeworks-starts-up-world-s-largest-direct-air-capture-plant/.
[8] Harzendorf F, et al. Criteria for effective site selection of direct air capture and storage projects. Environ Res Lett 2024;19(11).
[9] van der Spek M, et al. An ecosystem of carbon dioxide removal reviews - part 1: direct air CO_2 capture and storage. Energy Environ Sci 2025.
[10] Gebald C, et al. Single-component and binary CO_2 and H_2O adsorption of amine-functionalized cellulose. Environ Sci Technol 2014;48(4):2497–504.
[11] Stampi-Bombelli V, van der Spek M, Mazzotti M. Analysis of direct capture of $ ${\hbox {CO}}_{2}$$ from ambient air via steam-assisted temperature–vacuum swing adsorption. Adsorption 2020;26(7):1183–97.
[12] Young J, et al. The impact of binary water–CO_2 isotherm models on the optimal performance of sorbent-based direct air capture processes. Energ Environ Sci 2021;14(10):5377–94.
[13] Song A-Y, et al. Discerning molecular-level CO_2 adsorption behavior in amine-modified sorbents within a controlled CO_2/H_2O environment towards direct air capture. J Mater Chem A 2024;12(38):25875–86.
[14] Stuckert AN, Yang RT. CO_2 capture from the atmosphere and simultaneous concentration using zeolites and amine-grafted SBA-15. Environ Sci Technol 2011;45(23):10257–64.
[15] Veneman R, et al. Adsorption of H_2O and CO_2 on supported amine sorbents. Int J Greenhouse Gas Control 2015;41:268–75.
[16] Yu J, Chuang SSC. The Structure of Adsorbed Species on Immobilized Amines in CO_2 Capture: an in Situ IR Study. Energy Fuel 2016;30(9):7579–87.
[17] Sendi M, et al. Geospatial analysis of regional climate impacts to accelerate cost-efficient direct air capture deployment. One Earth 2022;5(10):1153–64.
[18] Wiegner JF, et al. Optimal design and operation of solid sorbent direct air capture processes at varying ambient conditions. Ind Eng Chem Res 2022;61(34):12649–67.
[19] Young J, et al. Process-informed adsorbent design guidelines for direct air capture. Chem Eng J 2023;456.
[20] Ji Y, et al. Solar-assisted temperature vacuum swing adsorption for direct air capture: effect of relative humidity. Appl Energy 2023;348.
[21] Postweiler P, et al. Environmental process optimisation of an adsorption-based direct air carbon capture and storage system. Energ Environ Sci 2024;17(9):3004–20.
[22] Rezo D, et al. A method for siting adsorption-based direct air carbon capture and storage plants for maximum CO2 removal. Carbon Neutr 2024;3(1).
[23] Zhang Z, et al. Multi-dimensional process optimization of temperature-vacuum swing adsorption for CO_2 capture from humid air. Energy 2025;334.
[24] Luukkonen A, Elfving J, Inkeri E. Improving adsorption-based direct air capture performance through operating parameter optimization. Chem Eng J 2023;471.
[25] Schellevis HM, van Schagen TN, Brilman DWF. Process optimization of a fixed bed reactor system for direct air capture. Int J Greenhouse Gas Control 2021;110.
[26] Zhu X, et al. Design of steam-assisted temperature vacuum-swing adsorption processes for efficient CO_2 capture from ambient air. Renew Sustain Energy Rev 2021;137.
[27] Sanz-Perez ES, et al. Direct capture of CO_2 from ambient air. Chem Rev 2016;116(19):11840–76.
[28] Low M-Y, et al. Analytical review of the current state of knowledge of adsorption materials and processes for direct air capture. Chem Eng Res Des 2023;189:745–67.
[29] Bouaboula H, et al. Comparative review of direct air capture technologies: from technical, commercial, economic, and environmental aspects. Chem Eng J 2024;484.
[30] PRODUKTINFORMATION LEWATIT® VP OC 1065. 2025, LANXESS Deutschland GmbH.
[31] Wenzel H, et al. Towards water-conscious green hydrogen and methanol production: a techno-economic review. Nexus 2025;2(1).
[32] McQueen N, et al. A review of direct air capture (DAC): scaling up commercial technologies and innovating for the future. Prog Energy 2021;3(3).
[33] Terlouw T, et al. Assessment of potential and techno-economic performance of solid sorbent direct air capture with CO_2 storage in Europe. Environ Sci Technol 2024;58(24):10567–81.
[34] Sendi M, et al. Geospatial techno-economic and environmental assessment of different energy options for solid sorbent direct air capture. Cell Rep Sustain 2024;1(8):100151.
[35] Wenzel H, et al. Weather conditions severely impact optimal direct air capture siting. Adv Appl Energy 2025;19:100229.
[36] Deschamps T, et al. Modeling of vacuum temperature swing adsorption for direct air capture using aspen adsorption. Clean Technol 2022;4(2):258–75.
[37] Aspen Adsorption. 2020, Aspen Technology Inc.: Bedford, MA, USA.
[38] Sonnleitner E, Schöny G, Hofbauer H. Assessment of zeolite 13X and Lewatit® VP OC 1065 for application in a continuous temperature swing adsorption process for biogas upgrading. Biomass Convers Biorefin 2017;8(2):379–95.
[39] Bos MJ, et al. Study on transport phenomena and intrinsic kinetics for CO_2 adsorption in solid amine sorbent. Chem Eng J 2019;377.
[40] AspenTech, Aspen Adsorption and Aspen Chromatography. 2025.
[41] Bajamundi CJE, et al. Capturing CO_2 from air: technical performance and process control improvement. J CO2 Util 2019;30:232–9.
[42] Heydari-Gorji A, Sayari A. Thermal, oxidative, and CO_2-induced degradation of supported polyethylenimine adsorbents. Ind Eng Chem Res 2012;51(19):6887–94.
[43] Gebald, C.M., W.; Repond, N.; Ruesch, T.; Wurzbacher, J., Direct air capture device. 2015: United States.
[44] Wu X, Krishnamoorti R, Bollini P. Technological options for direct air capture: a comparative process engineering review. Annu Rev Chem Biomol Eng 2022;13:279–300.
[45] MATLAB. 2024, The MathWorks, Inc.: Natick, MA, USA.
[46] Hamedi H, Brinkmann T, Wolff T. Techno-economic assessment of H2 extraction from natural gas distribution grids: a novel simulation-based optimization framework for pressure swing adsorption processes. Chem Eng J Adv 2023;16.
[47] Hersbach H, et al. The ERA5 global reanalysis. Q J R Meteorolog Soc 2020;146(730):1999–2049.
[48] Project Cypress. 06.06.2025]; Available from: https://projectcypress.com/.
[49] IEA, Global Hydrogen Review. 2024, IEA: Paris.

[50] IRENA, Global hydrogen trade to meet the 1.5°C climate goal: Part III – Green hydrogen cost and potential. 2022, International Renewable Energy Agency: Abu Dhabi.
[51] Ryberg DS, et al. The future of European onshore wind energy potential: detailed distribution and simulation of advanced turbine designs. Energy 2019;182:1222–38.
[52] Winkler C, et al. Participatory mapping of local green hydrogen cost-potentials in Sub-Saharan Africa. Int J Hydrogen Energy 2025;112:289–321.
[53] 2023 Electricity ATB Technologies. 2023 [cited 2025 08.12.]; Available from: https://atb.nrel.gov/electricity/2023/technologies.
[54] Grosse, R.C., B.; Stefan, W.; Geyer, R.; Robbi, S., Long term (2050) projections of techno-economic performance of large-scale heating and cooling in the EU. 2017, Publications Office of the European Union.
[55] Klütz T, Ethos.fine,, et al. A framework for integrated energy system assessment. J Open Source Software 2025;10(105).
[56] Leonzio G, Fennell PS, Shah N. A comparative study of different sorbents in the context of direct air capture (DAC): evaluation of key performance indicators and comparisons. Appl Sci 2022;12(5).
[57] Fasihi M, Efimova O, Breyer C. Techno-economic assessment of CO_2 direct air capture plants. J Clean Prod 2019;224:957–80.
[58] Hoffmann M, et al. A review of mixed-integer linear formulations for framework-based energy system models. Adv Appl Energy 2024;16.
[59] Selmert V, et al. Overcoming the energy–water nexus in dry regions – water-positive production of green hydrogen carriers and base chemicals: the DryHy project – technical aspects. Sustainable Energy Fuels 2025;9(7):1672–82.
[60] Wang Y, et al. Distributed direct air capture of carbon dioxide by synergistic water harvesting. Nat Commun 2024;15(1):9745.
[61] Gislason SR, et al. Mineral sequestration of carbon dioxide in basalt: a pre-injection overview of the CarbFix project. Int J Greenhouse Gas Control 2010;4(3):537–45.
[62] Ragnheidardottir E, et al. Opportunities and challenges for CarbFix: an evaluation of capacities and costs for the pilot scale mineralization sequestration project at Hellisheidi, Iceland and beyond. Int J Greenhouse Gas Control 2011;5(4):1065–72.